Chemical Science

ROYAL SOCIETY OF CHEMISTRY

EDGE ARTICLE

View Article Online
View Journal | View Issue

Cite this: *Chem. Sci.*, 2025, **16**, 5918

All publication charges for this article have been paid for by the Royal Society of Chemistry

Received 22nd January 2025
Accepted 26th February 2025

DOI: 10.1039/d5sc00591d

rsc.li/chemical-science

A sequential esterification-ring closing metathesis-Nozaki–Hiyama–Kishi strategy for constructing a natural product-like library of tetrahydrofuran-containing macrolides†

Daniel Driedger,‡ Darryl M. Wilson‡ and Robert Britton *

Polyketide-like macrolides (pMLs) represent a privileged class of compounds with a high incidence of bioactivity, however their structural complexity challenges their synthesis and more general study. Here we report the synthesis of a library of tetrahydrofuran-containing pMLs underpinned by a robust and convergent build/couple/pair/couple synthetic approach. The library comprises 170 pMLs originating from 17 building blocks, 10 of which were synthesized using a proline-catalyzed α-chlorination aldol reaction. Northern and southern hemisphere building blocks were coupled using either an oxidation/Horner-Wadsworth-Emmons sequence or a saponification/Steglich esterification strategy. Coupled fragments were cyclized *via* ring closing metathesis to yield macrocycles 14–16 atoms in size, which we diversified using 3 eastern side chain vinyl iodides through a Nozaki–Hiyama–Kishi reaction.

Introduction

Macrocycles (rings ≥12 atoms in size) are increasingly recognized as valuable frameworks in drug discovery due to their ability to bind to low-druggability targets, including the disruption of protein–protein interactions (PPIs).[1,2] The unique binding of macrolides to protein surfaces benefits from numerous functional groups strategically displayed over a large surface area and a conformational pre-organization provided by the macrocyclic skeleton.[3] Despite often violating established drug-like physicochemical rules, macrocycles also display surprisingly effective pharmacokinetic properties and cellular uptake, which has been attributed in part to their ability to temporarily mask polar groups through conformational interconversions.[3,4] Therefore, it is no surprise that >80 macrocyclic compounds have been approved as drugs, most of which are derived from natural products,[1,5] and the discovery of new bioactive macrocycles remains an important field of research.[2]

Among the several sub-categories of macrocyclic natural products are polyketide-like macrolides (pMLs), distinguished by a macrocyclic lactone often containing contiguous methyl and hydroxyl groups, and unsaturations consistent with natural products produced *via* polyketide synthases (Fig. 1). pMLs are abundant in nature, representing 6% of all microbial secondary metabolites, and over-represented among approved macrocyclic drugs.[1,6,7] Aside from natural product isolation campaigns, the discovery of new pMLs is challenged by the demanding total synthesis campaigns required for their production[8–10] as well as the scarcity of compound libraries that approach the complexity of such compounds.[11,12]

Recently, we reported a strategy termed the Targeted Sampling of Natural Product space (TSNaP)[13] that was designed to identify and assess regions of chemical space bounded by tetrahydrofuran-containing macrolides (Fig. 2A).[14] Using TSNaP, we computationally assembled a collection of virtual pMLs using pML-inspired building blocks. We then prioritized

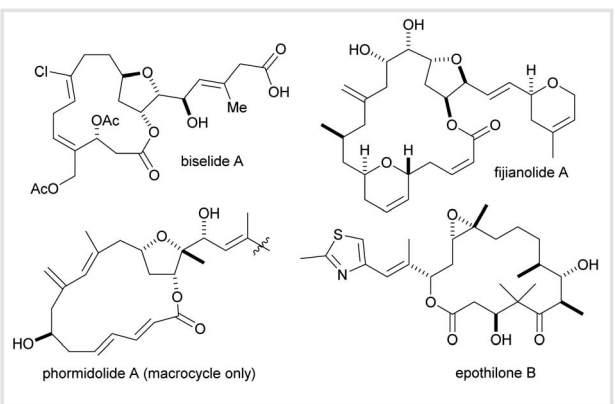

Fig. 1 A selection of polyketide-like macrolide natural products. Biselide A, fijianolide A, and phormidolide A are also classified as THF-containing macrolides.

Department of Chemistry, Simon Fraser University, Burnaby, British Columbia, V5A 1S6, Canada. E-mail: rbritton@sfu.ca

† Electronic supplementary information (ESI) available. See DOI: https://doi.org/10.1039/d5sc00591d

‡ Contributed equally.

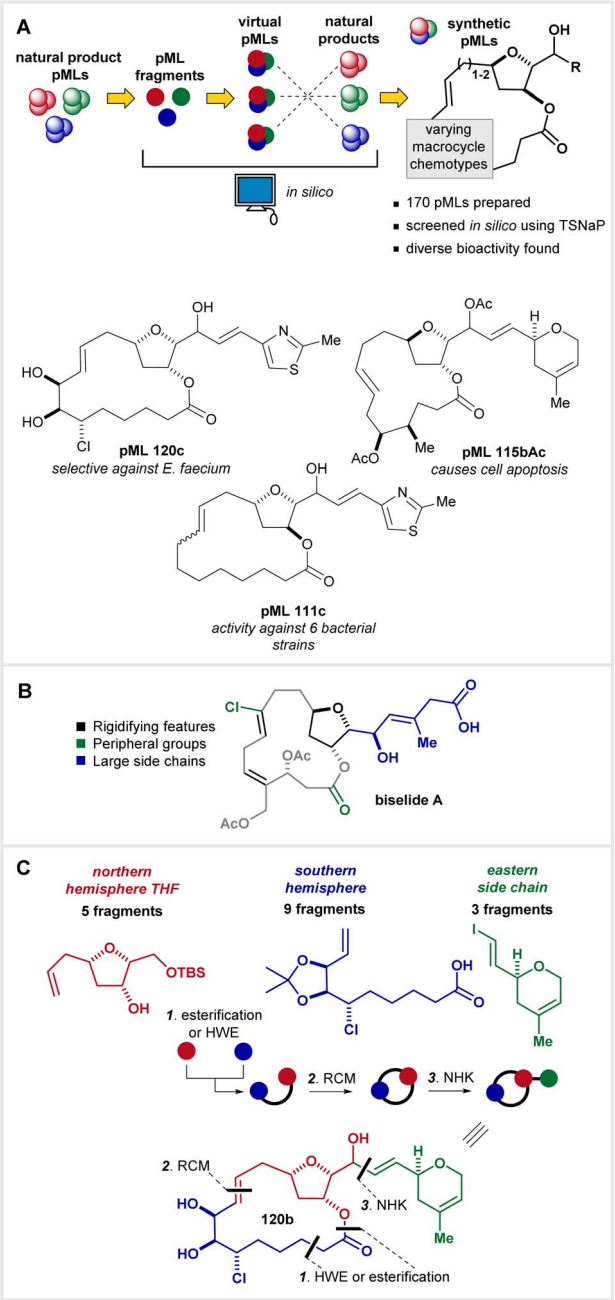

Fig. 2 (A) Summary of the TSNaP approach and a sample of hit molecules from the biological testing. (B) Conserved features amongst bioactive macrocycles as highlighted in biselide A. (C) Our generalized strategy for the assembly of the pML library.

the virtual pMLs according to similarity scores with natural THF-containing macrolides (*e.g.*, biselide A, fijianolide A, phormidolide A, Fig. 1) and synthesized a library of 170 tetrahydrofuran-containing pMLs based on their similarity scores. Finally, we screened this library in a panel of whole-cell biological assays, revealing hit rates exceeding those typically encountered in small molecule libraries. Hits included antibacterial pMLs **120c** and **111c**, as well as pMLs such as **115Ac** which showed an activity profile similar to that of known apoptosis-inducing compounds (Fig. 2A). Considering the wide scope of the TSNaP study, our initial report placed an emphasis on the rationale behind the library design, our process for selecting target compounds, and the results from biological testing of the library. Here, we instead disclose the entire breadth of the library synthesis, which represented a considerable effort (>300 synthetic steps) made possible by a handful of powerful synthetic methods and a convergent approach. We also discuss the synthetic challenges encountered in assembling such a pML library, and highlight useful insights gained from this synthesis campaign.

Results and discussion

Synthetic strategy

Applying the TSNaP approach, the pML library members were designed to fulfill a number of the key criteria attributed to bioactive macrocycles by Whitty.[3] These are exemplified in the natural product biselide A (Fig. 2B) and include: (i) rigidifying groups such as embedded rings and unsaturations, (ii) diverse heavy atom peripheral groups (*e.g.*, OH, CH_3, Cl), and (iii) one or more large substituents or side chains attached to the macrocycle. Each of these elements are accounted for amongst the 3 classes of building blocks used in the library synthesis, coupled together in various combinations using a build-couple-pair-couple (B/C/P/C) strategy.[15,16] The northern hemisphere THF (5 distinct fragments, red, Fig. 2C), the southern hemisphere (9 distinct fragments, blue), and the eastern side chain (3 distinct fragments, green) comprise the assortment of library building blocks. After preparing all fragments ("build"), one of the five tetrahydrofuranols (differing in stereochemistry and chain length) was joined ("couple") to a southern hemisphere enoic aldehyde or acid using either a Horner–Wadsworth–Emmons (HWE) reaction (for enoic aldehydes: 1st-generation approach) or a Steglich esterification (for enoic acids: 2nd-generation approach). Both approaches provided equivalent substrates for the subsequent ring closing metathesis (RCM) reaction to form a macrocycle ("pair"). After deprotection and oxidation of the northern tetrahydrofuranol, the material was divided into 3 portions, and a Nozaki–Hiyama–Kishi (NHK) reaction was used to join each of the 3 eastern side chain vinyl iodides with the macrocyclic aldehyde ("couple"). The synthesis of each individual library member was accomplished after the deprotection of any alcohols contained within the macrocycle, providing 3 library members per assembly sequence. This convergent and combinatorial B/C/P/C approach allowed us to generate a large library of pMLs with a reduced total step count and only a handful of building blocks (17 in total).

Synthesis of northern hemisphere THF building blocks

With an aim of achieving a balance between similarity and dissimilarity from known THF-macrolide natural products and targeting 'natural product-like' chemical space, the stereochemistry of the tetrahydrofuranol series **1a–e** (Fig. 3A) was chosen to overlap with that of the biselides,[17] fijianolides (laulimalides),[18,19] and phormidolide A (Fig. 1).[20] With this

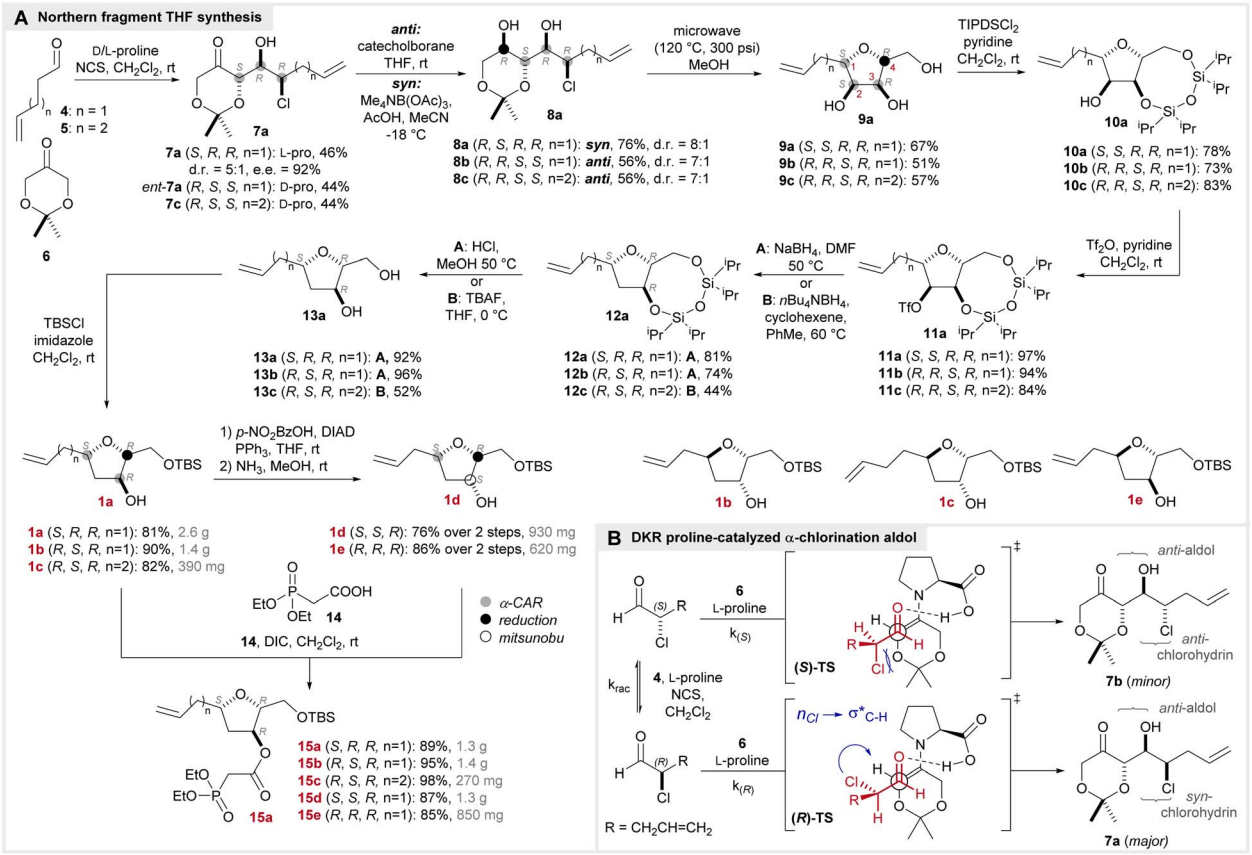

Fig. 3 (A) Syntheses of northern hemisphere THF building blocks. (B) Scheme for the DKR proline-catalyzed α-CAR (α-chlorination aldol reaction).

challenge in mind, we relied on the proline-catalyzed α-chlorination aldol reaction (α-CAR) to create the northern THF fragments (Fig. 3B). This robust and scalable methodology was developed previously in our lab[21,22] and has proven effective for the synthesis of many chloropolyols, which are excellent precursors to ribose analogues, carbohydrates and iminosugars.[23–26] Notably, this process involves a dynamic kinetic resolution (DKR) and uses inexpensive D/L-proline and readily available achiral starting materials such as pent-4-enal (**4**) and 2,2-dimethyl-1,3-dioxan-5-one (**6**) to establish the 4 contiguous THF stereocentres in only 2 steps with high enantioselectivity and operational ease, enabling large scale parallel syntheses of early intermediates on multi-gram scale. Moreover, several of these early intermediates serve dual purpose in creating both northern and southern hemisphere building blocks. Each of the 8 possible stereoisomers (each resembling a 2-deoxy furanose, see **9a** for numbering conventions) could be targeted by making binary decisions at 3 junctions: (i) the use of either L- or D-proline for the α-CAR (determines C1), (ii) either a 1,3-*anti* or 1,3-*syn* reduction of the resulting chlorohydrin (determines C4), and (iii) an optional Mitsunobu inversion of the exposed alcohol in **1a–c** (determines C3).

The tetrahydrofuranol synthesis is displayed in Fig. 3A, and begins with the aforementioned α-CAR between 2,2-dimethyl-1,3-dioxan-5-one (**6**) and either pent-4-enal (**4**) or hex-5-enal (**5**) to provide chlorohydrins **7a**, *ent*-**7a**, and **7c** in 44–46% yield (5 : 1 dr, 92% ee for **7a**).[21] Either an Evans–Saksena reduction[27] or catecholborane reduction[28] yielded diols **8a–c** stereoselectively with yields of 56–76%. A microwave promoted cyclization involving the newly reduced alcohol and the secondary alkyl chloride delivered furan triols **9a–c** in yields of 51–67%. The design of our library necessitated the deoxygenation of the C2 alcohol, to which the next 4 steps were dedicated, beginning with a selective protection using $TIPDiSiCl_2$ (ref. 29) to yield alcohols **10a–c** in good yield (73–83%). Triflation was followed by deoxygenation initially using nBu_4NBH_4/cyclohexene (**12c**, 44%) and after further optimization, $NaBH_4$ (**12a** in 74%, **12b** in 81% yield). The disiloxane protecting group was removed with either TBAF/THF at 0 °C (**13c**, 52%) or HCl/MeOH at 50 °C (**13a** in 92%, **13b** in 96% yield) followed by selective re-protection using TBSCl/imidazole to furnish the first set of functional building blocks, **1a**, **1b**, and **1c** in excellent yield (81–90%). C3 epimers **1d** and **1e** could be produced *via* a Mitsunobu inversion 2-step sequence using *p*-nitrobenzoic acid[30] (76% and 86% yield over 2 steps, respectively). For our 1st-generation approach (*vide infra*), **1a–e** were esterified with diethylphosphonoacetic acid (**14**) and DIC to complete the HWE-ready set of northern THF fragments **15a–e** in excellent yield (85–98%). Overall, the 8–10 step sequence offered a stereochemically flexible and straightforward path toward ample quantities of 5 northern THF building blocks (>1 g in some cases).

Synthesis of southern hemisphere building blocks

Next, we turned our attention to the synthesis of the southern hemisphere fragments. Our intention for these fragments was to include a variety of pML peripheral groups (Me, OH, Cl) with differences in substitution pattern and stereochemistry, along with the following constraints required for incorporation into the envisioned macrocycles: (i) 6–10 carbons in length for optimal macrocycle ring size, (ii) a terminal alkene for RCM, and (iii) a terminal aldehyde or carboxylic acid for either an HWE reaction or Steglich esterification, respectively.

We began by making use of the dual purpose THF-containing fragments **16a** (13% from **8a**) and **16b** (18% from **8b**) which were convenient acetonide-protected side-products of the microwave cyclization reactions from the northern THF fragment syntheses (Fig. 4A). Oxidation using Dess–Martin periodinane[31] followed by a HWE reaction using Masamune–Roush conditions[32] and triethylphosphonoacetate (**17**) afforded α,β-unsaturated esters **18a** and **18b** (68% and 72% over 2 steps). These two southern fragments were finalized *via* reduction using Stryker's reagent[33,34] yielding esters **2a** (32%) and **2b** (55%), each only 3 additional steps from material in-hand.

Our next targets were chlorinated fragments based on manipulations of the keto-chlorohydrins **7a** and **7c** from the northern THF fragment synthesis. Treatment with $InBr_3$ in anhydrous MeCN caused a migration of the 1,3-acetonide to the

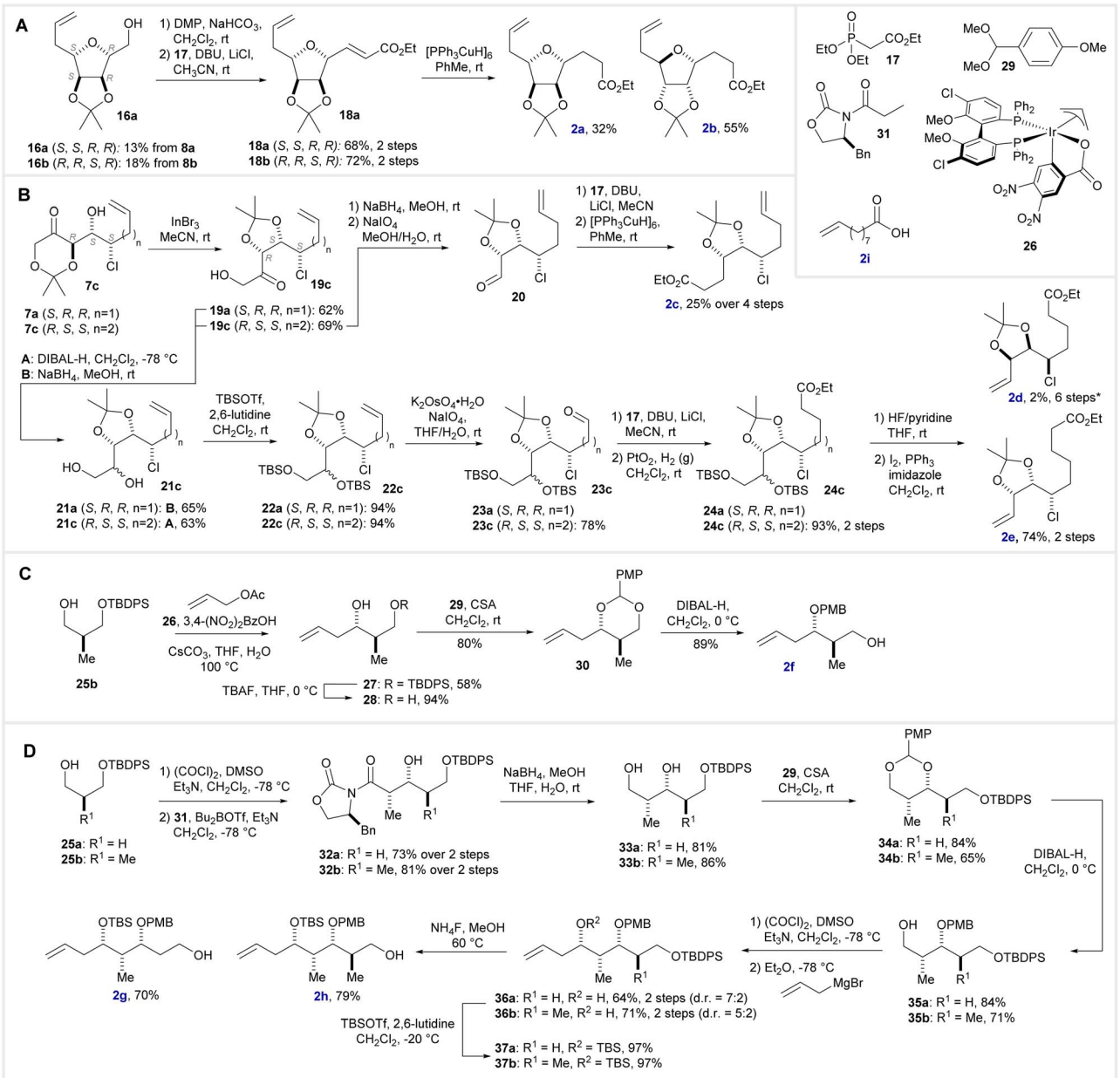

Fig. 4 (A) Syntheses of THF-containing southern fragments **2a** and **2b**. (B) Syntheses of chloro-diol southern fragments **2c**, **2d**, and **2e**. (C) Synthesis of southern fragment **2f**. (D) Syntheses of southern fragments **2g** and **2h**. *Yield corresponds to the carboxylic acid product of an additional saponification step.

1,2-acetonide delivering acyloins **19a** and **19c** (62% and 69% yields, respectively). Reduction of **19c** with $NaBH_4$ produced an inconsequential diastereomeric mixture of diols that was then cleaved with $NaIO_4$ to give the intermediate aldehyde **20**. The same HWE-Stryker's sequence from the synthesis of **2a** and **2b** yielded the completed enoic ester **2c** in 25% over 4 steps from **19c** (Fig. 4B). Unfortunately, it would later be found that this southern hemisphere fragment had a tendency to undergo trans-esterification after or during the deprotection of the final macrocyclic products (see **119a–c**, Chart 1) due to the proximity of the alcohol to the ester (γ-lactone formation).

Not wanting to abandon the chloride-containing building blocks, we devised a synthesis of two related building blocks (**2d** and **2e**) that exchanged the positions of the terminal alkene and ester, shifting the alcohols further away from the ester while retaining the chloride function (Fig. 4B). For the synthesis of **2e**, DIBAL-H was used to reduce acetonide-migrated intermediate **19c** in 63% yield. The mixture of diastereomeric diols (**21c**) was carried forward and silylated with TBSOTf/2,6-lutidine to give **22c** in excellent yield (94%). Oxidative cleavage of the alkene function by means of catalytic $K_2OsO_4 \cdot 2H_2O$ in the presence of $NaIO_4$ proceeded smoothly to deliver aldehyde **23c** in 78% yield. Next, olefination of aldehyde **23c** with phosphonate **17** using an HWE reaction followed by hydrogenation (H_2/PtO_2) of the resultant α,β-unsaturated ester delivered saturated ester **24c** in 93% yield over 2 steps. Finally, desilylation with HF/pyridine followed by a Garegg–Samuelsson olefination[35] of the resultant diol cleanly afforded ester **2e** (74% over 2 steps). Ester **2d** was produced using an analogous route from acyloin **19a**, and despite dramatically reduced yields (2% over 6 steps), enough material was available for incorporation into a set of 3 macrocycles.

To supplement the collection of southern fragments originating from the α-CAR chemistry, we also generated 3 enoic alcohols using alternative methods for synthesizing polyketide-like motifs. The simplest of these is PMB alcohol **2f** containing 2 adjacent stereocentres (Fig. 4C). The synthesis follows a route reported by Krische and co-workers,[36] beginning with a diastereoselective allylation of the silyl-protected alcohol **25b**, which proceeded in 58% yield. TBDPS deprotection of the resultant alcohol **27** (94%) followed by a PMB protection (80%) and reductive opening using DIBAL-H (89%) furnished primary alcohol **2f** in 39% over 4 steps.

The more complex fragments **2g** and **2h**, containing 3 and 4 stereocentres, respectively, required more onerous syntheses using an Evans-aldol strategy inspired by and overlapping with past syntheses (Fig. 4D).[36–40] Synthesis of **2g** began with the oxidation of mono-TBDPS protected propanediol **25a** (1 step from 1,3-propanediol) under Swern conditions.[41] The resultant crude aldehyde was immediately subjected to an Evans-aldol

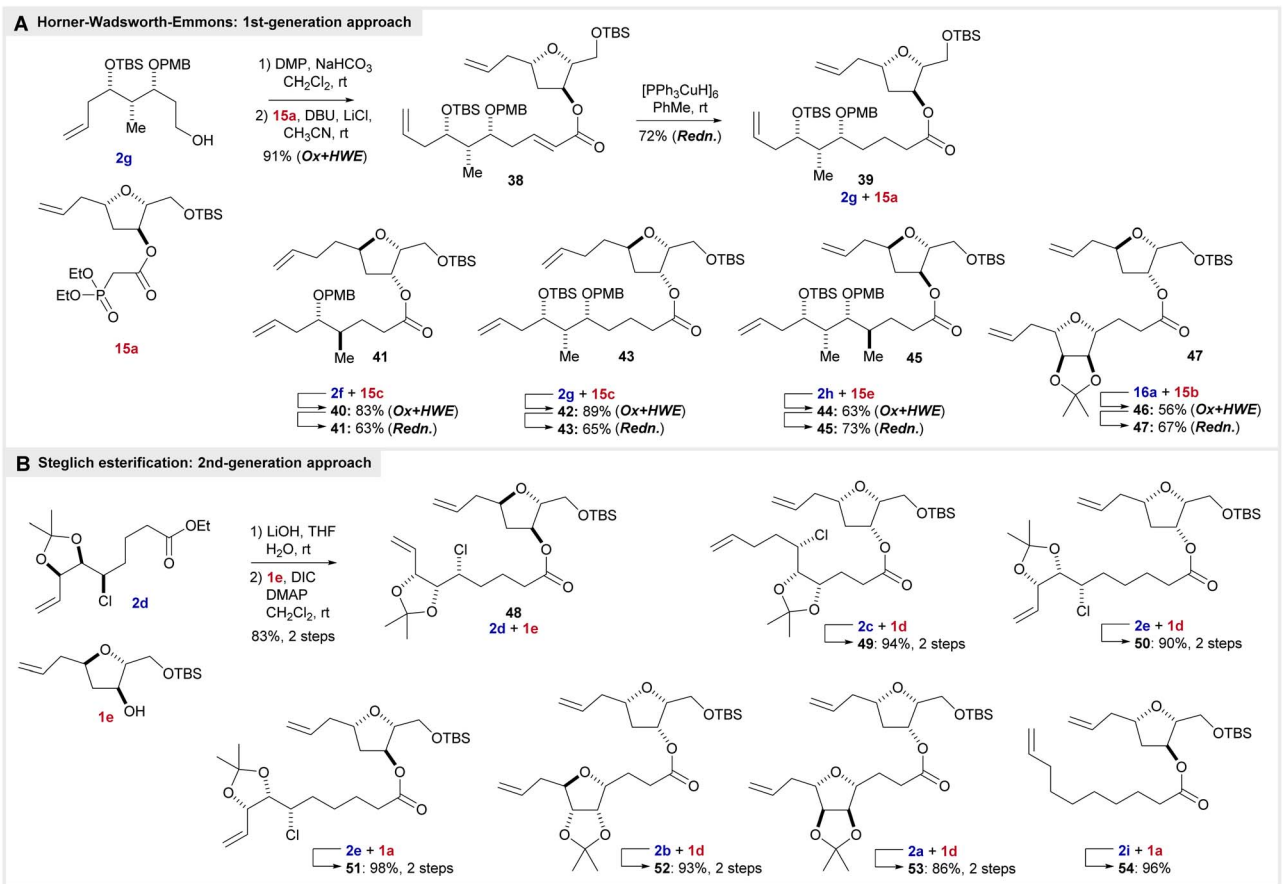

Fig. 5 (A) Oxidation of northern hemisphere THFs and HWE coupling with southern hemisphere fragments. (B) Saponification of northern hemisphere THFs and Steglich esterification coupling with southern hemisphere fragments.

reaction with the boron enolate produced from enolization of **31** with Bu_2BOTf/Et_3N,[37,42] affording *syn* aldol adduct **32a** in 73% yield over 2 steps. Next, **32a** was reduced with $NaBH_4$ in MeOH/H_2O (81%) followed by exposure to dimethyl acetal **29** in the presence of CSA to furnish acetal **34a** in 84% yield. Selective opening of the acetal with DIBAL-H gave PMB protected alcohol **35a** in 84% yield. Swern oxidation of the primary alcohol function followed by allylation of the resultant aldehyde with allyl magnesium bromide furnished **36a** as the major diastereomer (64% overall yield, 2 steps, d.r. = 7 : 2). Subsequent exposure of **36a** to TBSOTf/2,6-lutidine delivered protected polyol **37a**. Finally, selective deprotection of the primary OTBDPS group was achieved with NH_4F in warm (60 °C) MeOH[43] to deliver the southern hemisphere building block **2g** in 75% yield. The entire sequence was repeated to produce **2h** in similar fashion and yield using the Roche ester-derived methyl congener **25b** as a starting point (Fig. 4D).

The last of the 9 fragments for the southern hemisphere of the macrocycle library was commercially available 9-decenoic acid (**2i**), which was used in macrocycles that we envisioned would act as a control or baseline to highlight the importance of the peripheral groups as it pertains to biological activity.

Coupling of northern and southern fragments

With all northern hemisphere THF and southern hemisphere fragments completed, we began the process of macrocycle assembly by combining fragments in unique combinations. Our 1st-generation coupling strategy involved an HWE reaction between one of phosphonates **15a–e** and enoic aldehydes derived from alcohols **2e**, **2f**, **2g**, and **16a**. As exemplified by the coupling of alcohol **2g** with phosphonate **15a** (Fig. 5A), the alcohol first undergoes oxidation *via* Dess–Martin periodinane, followed by an HWE reaction with **15a** under Masamune–Roush conditions.[32] All reactions proceed fairly smoothly with yields of 56–91%. Later it was discovered that the additional degree of unsaturation due to the newly formed α,β-unsaturated ester was detrimental to the success of the downstream ring closing metathesis (*vide infra*), therefore, the olefin was selectively reduced using Stryker's reagent, providing the coupled products **39**, **41**, **43**, **45**, and **47** in moderately good yield (65–87%).

The 1st-generation HWE approach was originally devised for facile use of keto-chlorohydrin products (such as **7a–c**) as southern hemisphere fragments and coupling partners. However, once it became clear that the keto-chlorohydrins were not compatible the RCM and that a reduction of the newly formed double bond was necessary, a 2nd-generation coupling strategy was devised. In the revised approach, we performed an HWE/reduction sequence on southern fragment aldehydes in advance, using triethyl phosphonoacetate (**17**) (see the synthesis of **2a–2e**, Fig. 4), and after reduction then saponification, we obtained carboxylic acids which could be esterified with northern THF alcohols **1a–e**. Overall, this bypassed the inclusion of the Stryker's reduction in the linear sequence as well as the phosphonate coupling step in the northern THF fragment synthesis, meanwhile providing the same molecular structures as would be produced *via* the 1st-generation approach.

The 2nd-generation strategy is exemplified by the coupling of enoic ester **2d** and THF alcohol **1e** (Fig. 5B). Ester **2d** underwent a saponification using LiOH in a mixture of THF and water, and the crude material was subjected to a Steglich esterification with alcohol **1e** using DIC as the coupling reagent to form ester **48** (83% over 2 steps). Using this method, esters **49–54** were also synthesized in excellent yields (86–98%) proving the 2nd-generation modification to be advantageous. All products obtained *via* the 1st and 2nd-generation coupling strategies could be used directly in the pivotal RCM reaction that would follow.

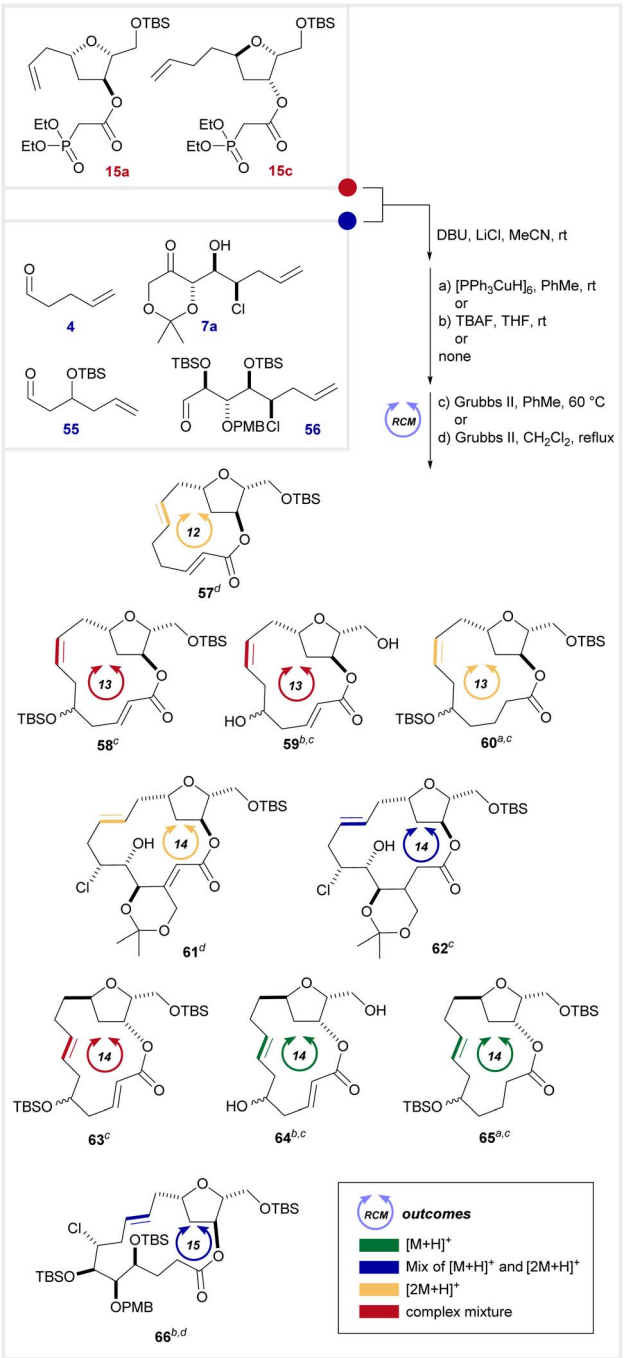

Fig. 6 RCM experiments to assess the formation of 12–15-membered rings, analyzed by HRMS.

Preliminary ring closing metathesis (RCM) experiments

To mitigate the risk associated with creating highly strained macrocycles, we designed an experiment to assess the viability of different southern hemisphere building blocks in RCM reactions with the goal of identifying both the ring-size and tolerated functionalities. This experiment began with preparing a handful of diene RCM precursors using the 1st-generation HWE coupling strategy (Fig. 6). THF phosphonates **15a** and **15c** were coupled to easily prepared aldehydes or ketones (pent-4-enal **4**, chlorohydrin **7a**, and aldehydes **55** and **56**) providing potential ring sizes of 12–16 atoms. Substrates were then optionally reduced (*via* Stryker's reagent) or deprotected (*via* TBAF) or neither, in order to study the effects of unsaturation and protecting groups on ring-closure. RCM results were analysed using high-resolution mass spectrometry (HRMS), which gave a qualitative picture of the reaction outcome including the formation or absence of product $[M + H]^+$ and the formation of the undesired homodimeric side-product $[2M + H]^+$.

Our first RCM experiment aimed to form the highly strained 12-membered macrocycle **57**, which unsurprisingly led to exclusive formation of macrocyclic homodimers. Similarly, attempted closure of the slightly larger 13-membered macrocycle series **58–60** was largely unsuccessful regardless of whether the alcohol function was protected (**58** *vs.* **59**) and the lactone was unsaturated or saturated (**58** *vs.* **60**). Attempted RCM to form the 14-membered macrocycle **61** led to exclusive formation of homodimeric macrocyclic products, however the successful RCM of the saturated congener **62** indicated that a reduction of the enoate function may promote ring closing in these systems. Motivated by this encouraging result, we reasoned that further alleviation of ring strain was required to enable facile formation of the desired monomeric macrocycles.

To ease ring strain, we attempted the formation of 14-membered macrocycle series **63–65** incorporating a less conformationally constrained southern hemisphere fragment. Disappointingly, the formation of 14-membered macrocycle **63** was not observed, however formation of desilylated congener **64** was detected, albeit in relatively small amounts and accompanied by several other unidentified products. Gratifyingly, saturated analogue **65** exclusively formed the desired RCM product, further indicating the importance of removing the C2–C3 olefin function. Finally, we evaluated formation of a heavily protected 15-membered macrocycle **66**, which resulted in formation of both the monomeric and homodimeric RCM products.

These results led to a few key conclusions: (i) the homodimer can be disfavoured by constructing macrocycles with a minimum ring size of 14 atoms, (ii) various peripheral functionalities are well tolerated, however, α,β-unsaturated esters should be avoided as they impart additional ring strain and/or cause competing undesired metathesis events, and (iii) limiting the use of bulky protecting groups is beneficial for the desired RCM processes. These insights allowed us to better predict which southern hemisphere fragments would be compatible in the key RCM reaction and therefore which building blocks should be prioritized for synthesis.

Synthesis of eastern fragment building blocks

The final set of building blocks to be synthesized was the eastern side chain fragment, each a vinyl iodide designed for an NHK coupling and modelled after side chains found in bioactive natural products. As such, we prioritized methyl amide **3a** that resembles the side chain found in haterumalides[44] and biselides,[17,45] dihydropyran **3b** that mimicked the side chain in the fijianolides[18,19] and thiazole **3c** found in the epothilones (Fig. 1, **3a–c** found in Fig. 7).[46]

Our efforts towards the syntheses of the side chains began with the methyl amide **3a** as outlined in Fig. 7. Here, but-2-ynol (**67**) was subjected to a known carboalumination–iodination to deliver vinyl iodide **68**[47] in good yield (80%), and the alcohol functionality was subsequently oxidized with chromic acid to furnish carboxylic acid **69** in 78% yield. Finally, treatment of acid **69** with DIC/HOBt generated the active ester *in situ*, which was then coupled with methylamine to furnish methyl amide **3a** in 54% yield.

The dihydropyran **3b** and thiazole **3c** side chains were prepared according to known sequences previously reported by

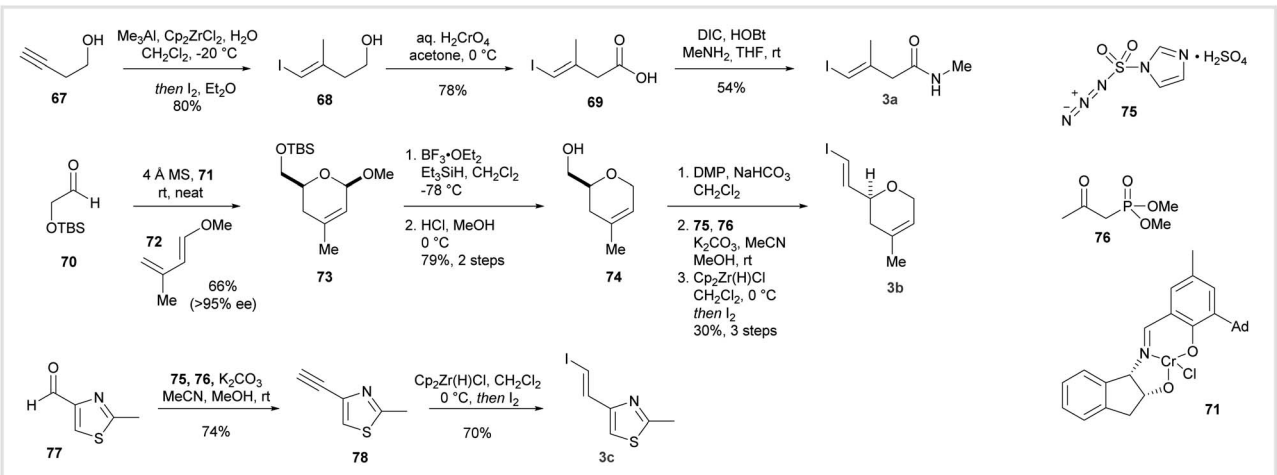

Fig. 7 Syntheses of the vinyl iodide-containing eastern fragments **3a–c**.

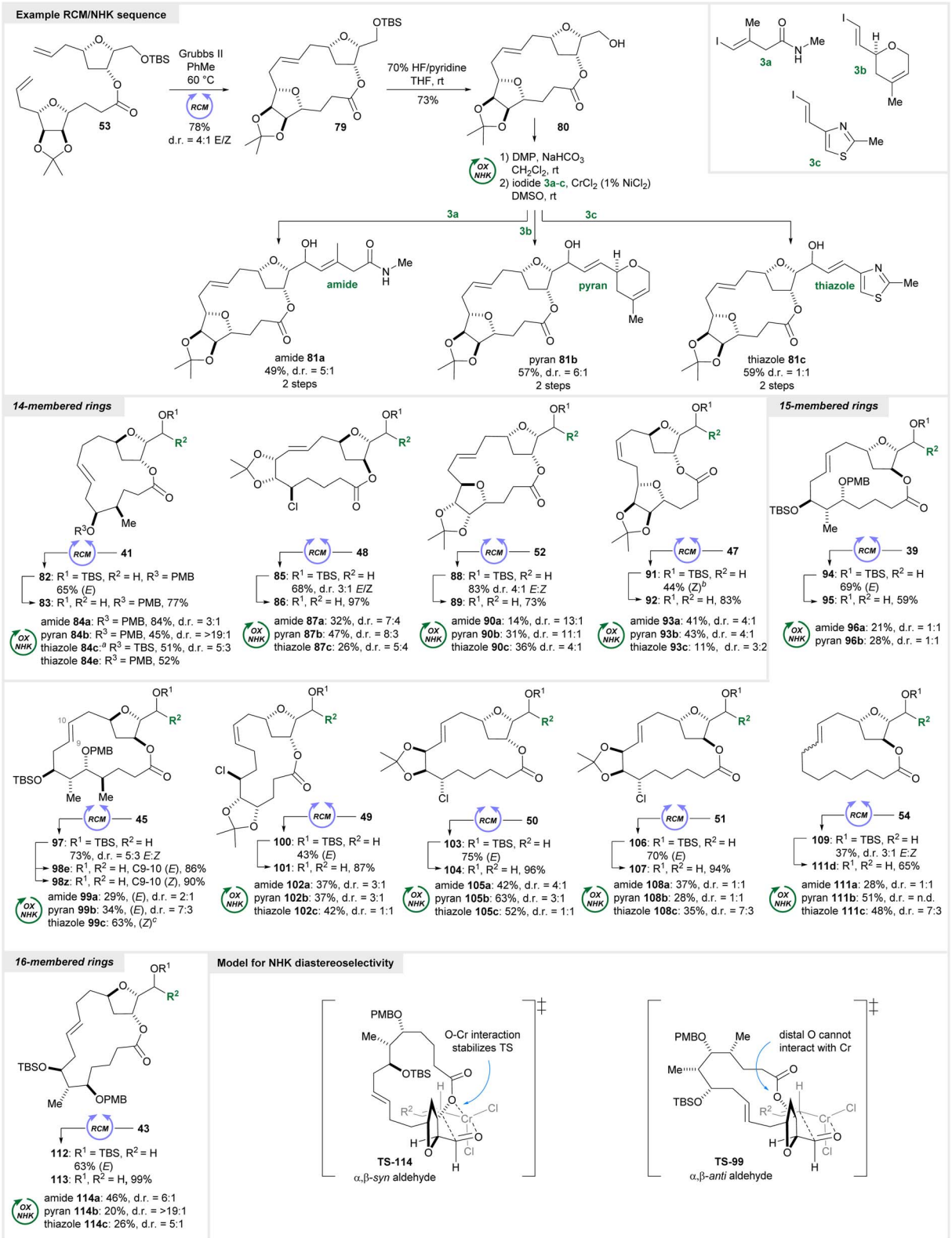

Fig. 8 RCM, TBS deprotection, oxidation, and NHK diversification of all macrocyclic precursors. [a]Thiazole **84c** made by subjecting to **82** to (1) DDQ, pH 7 buffer, CH_2Cl_2, rt and (2) TBSOTf, 2,6-lutidine, CH_2Cl_2, rt before undergoing 1° TBS deprotection and oxidation/NHK conditions as above. [b]Stewart-Grubbs catalyst. [c]d.r. not determined.

Paterson (Fig. 7).[48,49] Synthesis of dihydropyran **3b** initiated from a hetero-Diels–Alder (HDA) reaction[50,51] between TBS protected glycolaldehyde **70** and known diene **72** in the presence of Jacobsen's organochromium HDA catalyst **71** and proceeded smoothly to deliver **73** in 66% yield (>95% ee). Reduction of the methyl ether with $Et_3SiH/BF_3{\cdot}OEt_2$ and subsequent desilylation under acidic conditions (HCl/MeOH) gave primary alcohol **74** in 79% over both steps. Next, sequential Dess-Martin oxidation, homologation with the Ohira–Bestmann reagent (generated *in situ* from **75** and **76**), and hydrozirconation–iodination delivered vinyl iodide **3b** in 30% yield over 3 steps.

Via a related sequence, thiazole **3c** was prepared from commercially available **77** through homologation to furnish the desired alkyne **78** in 74% yield. Finally, hydrozirconation–iodination of alkyne **78** delivered vinyl iodide **3c** in 70% yield and concluded our efforts on the syntheses of the eastern side chains.

RCM and NHK coupling for diversification

With all fragments prepared, we turned to the critical juncture in the library synthesis, the RCM and NHK diversification sequence. An example sequence is illustrated in Fig. 8, starting from the diene **53**. A ring closing metathesis using Grubbs 2nd-generation catalyst heated to 60 °C in toluene afforded the macrocyclic product **79** in 78% yield with a d.r. of 4 : 1 *E*/*Z*. TBS deprotection with HF/pyridine produced **80** (73%) with its revealed exocyclic alcohol to be oxidized by Dess–Martin periodinane. In general, these macrocyclic aldehydes proved to be highly unstable, and the crude material was used immediately for the accompanying NHK reaction in all cases. Additionally, it was found that the use of freshly prepared Dess–Martin periodinane[31] aided in reducing the amount of hydrated aldehyde, which proved to be a major source of material loss. After oxidation of **80**, the resultant aldehyde was divided into 3 equal portions and coupled to each of the 3 eastern side-chain vinyl iodides *via* an NHK reaction.[52] Coupled products **81a–c** were isolated in moderate yield (49–59%) with a range of diastereomeric ratios (6 : 1 to 1 : 1). The 11 additional examples of the RCM/NHK sequence are summarized in Fig. 8, for a total of 12 sets of macrocyclic products (36 total products), and rings ranging from 14–16 atoms in size. In most cases, the RCM strongly favored the *E* macrocycle, with the exception of a few cases in which the *Z* isomer was formed in sufficient quantity to be used for the NHK coupling (**93a–c** and **99c**, Fig. 8). In general, the yields for the NHK were modest and in some cases low (<30%) with diastereomeric ratios covering the full range (1 : 1 to >19 : 1). In most cases, these diastereomers were inseparable by chromatography and were left as such. Additionally, we made the intentional decision to leave the stereochemistry of the diastereomeric alcohol unassigned, as determination of the configuration would require derivatization which would be complicated by limits in product supply at this point.

However, available literature on the NHK reaction suggests a modest, but clear, preference for the formation of the Felkin–Anh or polar Felkin–Anh products in acyclic[52–55] systems and some cyclic[56] systems. Notably, NHK couplings with tetrahydrofurfurals[57,58] including macrocyclic tetrahydrofurfurals[8,52,59] have been shown to proceed with a modest preference for the polar Felkin–Anh products. Thus, it is likely that where diastereoselectivity was observed, the major isomer is the polar Felkin–Anh product. Interestingly, when the stereocentres at positions C2 and C3 in the THF were *syn*-configured, the diastereoselectivity of the NHK was increased relative to comparable compounds in which these stereocentres were *anti*-configured (*e.g.*, compare d.r. for **105a–c** and **108a–c**). This enhanced selectivity is consistent with, and may arise from, a 4-coordinate[56,60] polar Felkin–Anh transition state where an oxygen atom of the *syn*-configured tetrahydrofurfural is capable of coordinating to the Cr(III) metal centre (Fig. 8). In contrast, a similar stabilizing interaction is not possible when the stereocentres at C2 and C3 are *anti*-configured, which may explain the poorer stereoselectivity in these cases. We note that this hypothesis about coordination in the *syn*-configured macrocyclic tetrahydrofurfurals remains speculative.

Final library member deprotections and acetylation

The final stage in the library synthesis was the deprotection of peripheral macrocyclic alcohols. Chart 1 pictures the entire macrocycle library, with any number of 3 deprotection conditions applied to each macrocycle. DDQ and pH 7 buffer in CH_2Cl_2 was used to remove the PMB group (conditions W), 70% HF/pyridine in THF was used to remove the TBS group (conditions X), and HCl in MeOH was used to remove the acetonide group from vicinal diols (conditions Y). The macrocyclic peripheral groups, determined by the southern hemisphere fragment, fall into 3 general categories: class I with stereogenic methyls (**115–118**), class II containing the chlorodiol (**119–122**), and class III consisting of an embedded tetrahydrofurandiol (**123–125**), plus the set of hydrocarbon macrocycles **111a–c** (class IV). Deprotections proceeded smoothly in most cases, however there were a few instances of undesired side-reactions. In the cases of **118c** and **119a–c** a translactonization occurred during the final deprotection to form a 5- or 6-membered lactone. Another anomaly in the library was the serendipitous oxidation of the allylic alcohol in substrate **84e** during oxidative deprotection of the PMB protecting group, providing **115e** as an additional library member (its alcohol congener was eventually made using a TBS-protected macrocycle, **115c**). Altogether, we were able to prepare 85 different macrocycles (including diastereomers). This includes the preparation of an analogue lacking a side-chain for each family of compounds, completing sets of 4 analogues per unique macrocycle. Additionally, many compounds represented a mixture of two NHK diastereomers which were both included in the total count.

To explore the effects of acetylation on bioactivity *via* cell permeability,[61,62] we also peracetylated a small portion (~1 mg of each compound (conditions Z)), to form **115–125Ac** and **111Ac**, doubling the count of library members to 170. As previously mentioned, the biological activity of this library was evaluated and discussed in detail in a recent publication.[13]

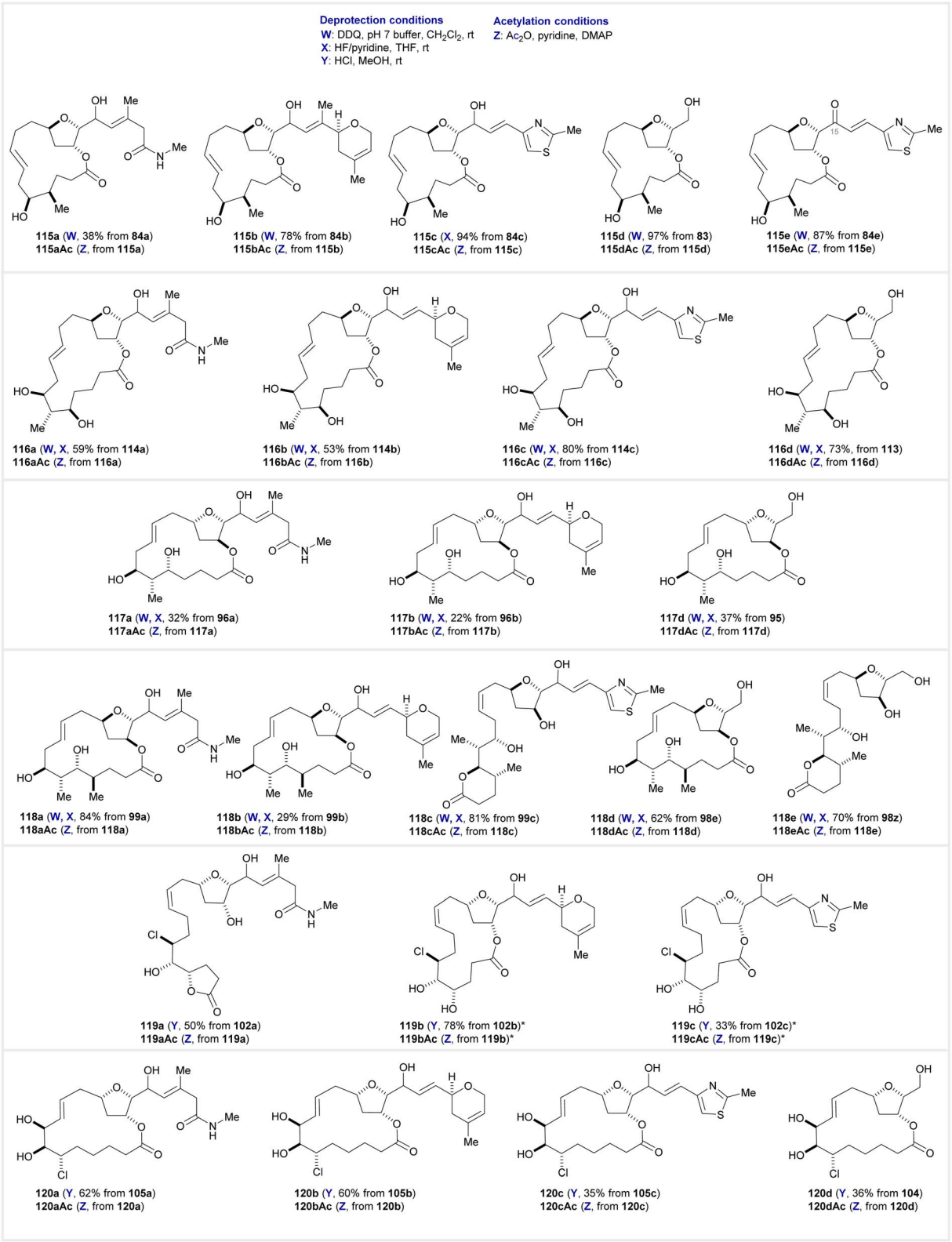

Chart 1 *Contd.*

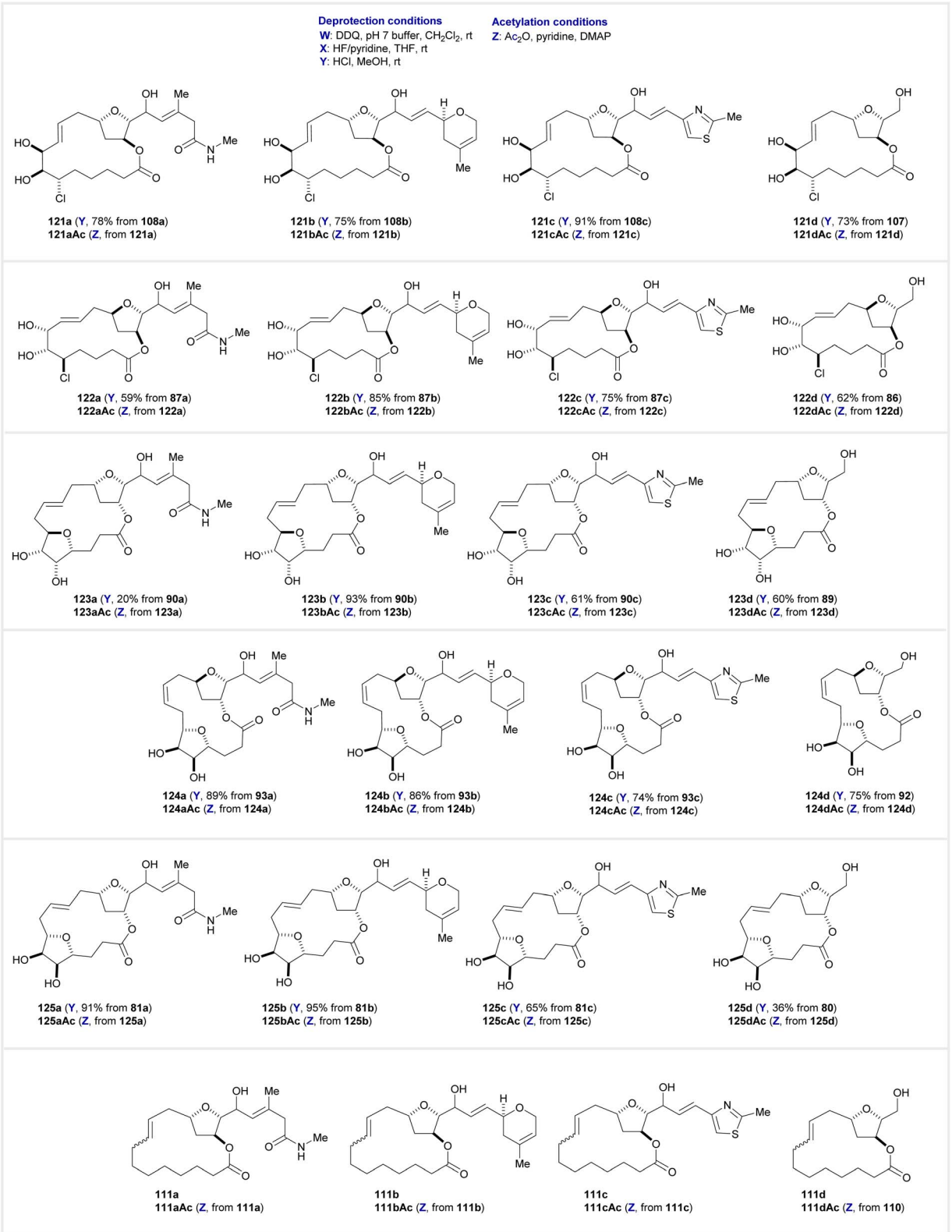

Chart 1 The completed macrolide library, with deprotection and acetylation yields below each structure. *Mix of macrocycle and translactone.

Conclusion

In summary, we synthesized a library of 170 pMLs varying in complexity, stereochemistry (6–9 stereocentres), ring size (14–16 atoms), peripheral groups (Me, OH, Cl, embedded THF), and large side-chains (amide, dihydropyran, and thiazole-containing). The synthetic campaign was enabled by numerous powerful synthetic methods, including the α-CAR reaction which was used to make 10 of the 14 chiral building blocks used in the library. Additionally, a compatibility screen of RCM reactions was used to guide library selection, followed by a challenging late-stage NHK reaction to diversify final products. We hope that the wide scope of reactions can act as a valuable resource for researchers, as well as provide a template for similar library syntheses to be accomplished on different families of molecules.

Data availability

The experimental procedures, characterization data and ^{1}H and ^{13}C NMR spectroscopic data generated in this study are provided in the ESI.†

Author contributions

D. D., D. M. W. and R. B. conceptualized the synthetic work, both D. D. and D. M. W. synthesized and characterized all compounds. Writing was done by D. D. and D. M. W. and supervision, funding acquisition, revision, and editing was done by R. B.

Conflicts of interest

There are no conflicts to declare.

Acknowledgements

Financial support from the Natural Sciences and Engineering Research Council (NSERC) of Canada was received by R. B. (Discovery Grant: 2019-06368), D. M. W. (CGS-M & PGS-D) and D. J. D. (CGS-M & CGS-D).

Notes and references

1 E. M. Driggers, S. P. Hale, J. Lee and N. K. Terrett, *Nat. Rev. Drug Discovery*, 2008, **7**, 608–624.
2 D. G. Jimenez, V. Poongavanam and J. Kihlberg, *J. Med. Chem.*, 2023, **66**, 5377–5396.
3 E. A. Villar, D. Beglov, S. Chennamadhavuni, J. A. Porco, D. Kozakov, S. Vajda and A. Whitty, *Nat. Chem. Biol.*, 2014, **10**, 723–731.
4 A. Whitty, M. Zhong, L. Viarengo, D. Beglov, D. R. Hall and S. Vajda, *Drug Discovery Today*, 2016, **21**, 712–717.
5 L. A. Viarengo-Baker, L. E. Brown, A. A. Rzepiela and A. Whitty, *Chem. Sci.*, 2021, **12**, 4309–4328.
6 P. Milton, J. I. D. Hamley, M. Walker and M. G. Basáñez, *Expert Rev. Anti-Infect. Ther.*, 2020, **18**, 1067–1081.
7 M. J. Yu, W. Zheng and B. M. Seletsky, *Nat. Prod. Rep.*, 2013, **30**, 1158–1164.
8 V. R. Challa, D. Kwon, M. Taron, H. Fan, B. Kang, D. Wilson, F. P. J. Haeckl, S. Keerthisinghe, R. G. Linington and R. Britton, *Chem. Sci.*, 2021, **12**, 5534–5543.
9 A. K. Ghosh and Y. Wang, *J. Am. Chem. Soc.*, 2000, **122**, 11027–11028.
10 S. A. May and P. A. Grieco, *Chem. Commun.*, 1998, 1597–1598.
11 Y. K. Kim, M. A. Arai, T. Arai, J. O. Lamenzo, E. F. Dean, N. Patterson, P. A. Clemons and S. L. Schreiber, *J. Am. Chem. Soc.*, 2004, **126**, 14740–14745.
12 I. B. Seiple, Z. Zhang, P. Jakubec, A. Langlois-Mercier, P. M. Wright, D. T. Hog, K. Yabu, S. R. Allu, T. Fukuzaki, P. N. Carlsen, Y. Kitamura, X. Zhou, M. L. Condakes, F. T. Szczypiński, W. D. Green and A. G. Myers, *Nature*, 2016, **533**, 338–345.
13 D. M. Wilson, D. J. Driedger, D. Y. Liu, S. Keerthisinghe, A. Hermann, C. Bieniossek, R. G. Linington and R. A. Britton, *Nat. Commun.*, 2024, **15**, 2534.
14 A. Lorente, J. Lamariano-Merketegi, F. Albericio and M. Álvarez, *Chem. Rev.*, 2013, **113**, 4567–4610.
15 T. E. Nielsen and S. L. Schreiber, *Angew. Chem., Int. Ed.*, 2008, **47**, 48–56.
16 K. T. Mortensen, T. J. Osberger, T. A. King, H. F. Sore and D. R. Spring, *Chem. Rev.*, 2019, **119**, 10288–10317.
17 T. Teruya, K. Suenaga, S. Maruyama, M. Kurotaki and H. Kigoshi, *Tetrahedron*, 2005, **61**, 6561–6567.
18 D. Corley, R. Herb, R. Moore and P. Scheur, *J. Org. Chem.*, 1988, **53**, 3644–3646.
19 E. Quiñoá, Y. Kakou and C. Phillip, *J. Org. Chem.*, 1988, **53**, 3642–3644.
20 R. T. Williamson, A. Boulanger, A. Vulpanovici, M. A. Roberts and W. H. Gerwick, *J. Org. Chem.*, 2002, **67**, 7927–7936.
21 M. Bergeron-Brlek, T. Teoh and R. Britton, *Org. Lett.*, 2013, **15**, 3554–3557.
22 M. Meanwell, G. Fehr, W. Ren, B. Adluri, V. Rose, J. Lehmann, S. M. Silverman, R. Rowshanpour, C. Adamson, M. Bergeron-Brlek, H. Foy, V. R. Challa, L. C. Campeau, T. Dudding and R. Britton, *Commun. Chem.*, 2021, **4**, 1–9.
23 A. Kaghad, D. Panagopoulos, G. Caballero-García, H. Zhai and R. Britton, *Nat. Commun.*, 2023, **14**, 1–8.
24 M. Bergeron-Brlek, M. Meanwell and R. Britton, *Nat. Commun.*, 2015, **6**, 1–6.
25 R. A. Ashmus, Y. Wang, M. González-Cuesta, D. T. King, B. Tiet, P. A. Gilormini, J. M. García Fernández, C. Ortiz Mellet, R. Britton and D. J. Vocadlo, *Org. Biomol. Chem.*, 2021, **19**, 8057–8062.
26 M. Meanwell, M. Sutherland and R. Britton, *Can. J. Chem.*, 2017, **96**, 144–147.
27 D. A. Evans, K. T. Chapman and E. M. Carreira, *J. Am. Chem. Soc.*, 1988, **110**, 3560–3578.
28 D. A. Evans and A. H. Hoveyda, *J. Org. Chem.*, 1990, **55**, 5190–5192.
29 W. T. Markiewicz, *Tetrahedron Lett.*, 1980, **21**, 4523–4524.
30 S. F. Martin and J. A. Dodge, *Tetrahedron Lett.*, 1991, **32**, 3017–3020.

31 D. B. Dess and J. C. Martin, *J. Org. Chem.*, 1983, **48**, 4155–4156.
32 M. A. Blanchette, W. Choy, J. T. Davis, A. P. Essenfeld, S. Masamune, W. R. Roush and T. Sakai, *Tetrahedron Lett.*, 1984, **25**, 2183–2186.
33 W. S. Mahoney, D. M. Brestensky and J. M. Stryker, *J. Am. Chem. Soc.*, 1988, **110**, 291–293.
34 D. W. Lee and J. Yun, *Tetrahedron Lett.*, 2005, **46**, 2037–2039.
35 J. Garegg and B. Samuelsson, *Synthesis*, 1976, **6**, 469–470.
36 D. C. Schmitt, A. M. R. Dechert-Schmitt and M. J. Krische, *Org. Lett.*, 2012, **14**, 6302–6305.
37 A. B. Smith, K. P. Minbiole, P. R. Verhoest and M. Schelhaas, *J. Am. Chem. Soc.*, 2001, **123**, 10942–10953.
38 T. K. Chakraborty, S. Ghosh and S. Dutta, *Tetrahedron Lett.*, 2001, **42**, 5085–5088.
39 T. K. Chakraborty and A. K. Chattopadhyay, *J. Org. Chem.*, 2008, **73**, 3578–3581.
40 A. T. Herrmann, T. Saito, C. E. Stivala, J. Tom and A. Zakarian, *J. Am. Chem. Soc.*, 2010, **132**, 5962–5963.
41 A. J. Mancuso, S. L. Huang and D. Swern, *J. Org. Chem.*, 1978, **43**, 2480–2482.
42 D. A. Evans, J. Bartroli and T. L. Shih, *J. Am. Chem. Soc.*, 1981, **103**, 2127–2129.
43 W. Zhang and M. J. Robins, *Tetrahedron Lett.*, 1992, **33**, 1177–1180.
44 N. Takada, H. Sato, K. Suenaga, H. Arimoto, K. Yamada, K. Ueda and D. Uemura, *Tetrahedron Lett.*, 1999, **40**, 6309–6312.
45 H. Kigoshi and I. Hayakawa, *Chem. Rec.*, 2007, **7**, 254–264.
46 K. Gerth, N. Bedorf, G. Höfle, H. Irschik and H. Reichenbach, *J. Antibiot.*, 1996, **49**, 560–563.
47 C. L. Rand, D. E. Van Horn, M. W. Moore and E. Negishi, *J. Org. Chem.*, 1981, **46**, 4093–4096.
48 I. Paterson, H. Bergmann, D. Menche and A. Berkessel, *Org. Lett.*, 2004, **6**, 1293–1295.
49 I. Paterson, D. Menche, A. E. Håkansson, A. Longstaff, D. Wong, I. Barasoain, R. M. Buey and J. F. Díaz, *Bioorg. Med. Chem. Lett.*, 2005, **15**, 2243–2247.
50 A. G. Dossetter, T. F. Jamison and E. N. Jacobsen, *Angew. Chem., Int. Ed.*, 1999, **38**, 2398–2400.
51 K. Gademann, D. E. Chavez and E. N. Jacobsen, *Angew. Chem., Int. Ed.*, 2002, **114**, 3185–3187.
52 A. Gil, F. Albericio and M. Álvarez, *Chem. Rev.*, 2017, **117**, 8420–8446.
53 M. D. Lewis and Y. Kishi, *Tetrahedron Lett.*, 1982, **23**, 2343–2346.
54 J. Mulzer, T. Schulze, A. Strecker and W. Denzer, *J. Org. Chem.*, 1988, **53**, 4098–4103.
55 J. Mulzer, L. Kattner, A. R. Strecker, C. Schröder, J. Buschmann, C. Lehmann and P. Luger, *J. Am. Chem. Soc.*, 1991, **113**, 4218–4229.
56 J. Pospíšil, C. Müller and A. Fürstner, *Chem.–Eur. J.*, 2009, **15**, 5956–5968.
57 J. Lamariano-Merketegi, A. Lorente, A. Gil, F. Albericio and M. Álvarez, *Eur. J. Org. Chem.*, 2015, 235–241.
58 A. Vinaykumar, B. Surender and B. V. Rao, *RSC Adv.*, 2023, **13**, 22824–22830.
59 I. Hayakawa, M. Ueda, M. Yamaura, Y. Ikeda, Y. Suzuki, K. Yoshizato and H. Kigoshi, *Org. Lett.*, 2008, **10**, 1859–1862.
60 D. W. C. Macmillan and L. E. Overman, *J. Am. Chem. Soc.*, 1995, **117**, 10391–10392.
61 M. Martínez-Martínez, C. Coscolín, G. Santiago, J. Chow, P. J. Stogios, R. Bargiela, C. Gertler, J. Navarro-Fernández, A. Bollinger, S. Thies, C. Méndez-García, A. Popovic, G. Brown, T. N. Chernikova, A. García-Moyano, G. E. K. Bjerga, P. Pérez-García, T. Hai, M. V. Del Pozo, R. Stokke, I. H. Steen, H. Cui, X. Xu, B. P. Nocek, M. Alcaide, M. Distaso, V. Mesa, A. I. Peláez, J. Sánchez, P. C. F. Buchholz, J. Pleiss, A. Fernández-Guerra, F. O. Glöckner, O. V. Golyshina, M. M. Yakimov, A. Savchenko, K. E. Jaeger, A. F. Yakunin, W. R. Streit, P. N. Golyshin, V. Guallar and M. Ferrer, *ACS Chem. Biol.*, 2018, **13**, 225–234.
62 J. Morstein, A. Capecchi, K. Hinnah, B. Park, J. Petit-Jacques, R. C. Van Lehn, J. L. Reymond and D. Trauner, *J. Am. Chem. Soc.*, 2022, **144**, 18532–18544.